On the Anisotropy of δ-Electrons from Slow Heavy-Ion Collisions in the Emission Angles ϑ_f and φ_f

D.H. Jakubaßa-Amundsen*

Physik-Department, Technische Universität München, Garching, Federal Republic of Germany

Within the united-atom perturbation theory, we have calculated the probability for the ejection of electrons from the K and L shells of heavy target atoms as a function of both polar and azimuthal angle of the electron. By including multipole transitions up to $l=2$, we found that for asymmetric collision systems and high electron energies the angular distribution has a dipole shape. For $s_{1/2}$ electrons, the dependence on the azimuthal angle varies strongly with impact parameter b, with a preference of electron ejection in the same direction as the scattered projectile for small b, and in the opposite direction for large b. This is in agreement with first experimental data.

1. Introduction

Since the early investigations on δ-electrons from heavy ion-atom collisions [1, 2] the spectroscopy of high-energy electrons has become established as a tool to study the properties of the bound electrons in the quasi-atomic system formed during the collision. In order to obtain not only information on the dependence of the electronic wavefunction on the absolute value of the momentum p, but also on its direction $\hat{p}$, an analysis of the *triple* differential cross section with respect to the projectile scattering angle ϑ and the energy E_f and direction ϑ_f and φ_f of the emitted electron is necessary. Such measurements in heavy systems have been proposed by Koenig and coworkers, and in addition to the specification of E_f and ϑ_f [1-3] first experiments have been carried out where also the dependence on the azimuthal angle φ_f at fixed scattering angles was determined [4]. This is a promising alternative to the recently applied method, where the spacial distribution of the atomic electrons can be obtained from a measurement of the angular distribution or polarisation of x-rays [5] or the angular distribution of Auger electrons [6] which are emitted when the electronic state after having been formed during the collision, decays into the ground state. However, in this kind of experiments a clear separation between

the formation and decay of the electronic state is implied [7] which excludes information on possible molecular properties of the initial state. On the other hand, the observation of the primary particles such as the δ-electrons, provides a source to study the initial state directly, but at the expense of a close coupling between the initial-state and the dynamical properties of the system. Both methods have in common the sensitivity of the angular distribution (or polarisation) to the relative phases of the transition amplitudes for forming the excited state.

For the theoretical description of δ-electron emission the semiclassical treatment is commonly in use [8]. For fast or very asymmetric collisions, atomic perturbation theory can be applied [9-11] and has been extended to describe the angular distribution of the emitted electrons [12]. For slow, less asymmetric collisions a molecular picture is appropriate, where the electrons are described by means of eigenstates of the two-center field of the target and projectile nucleus. However, calculations of this kind have only been performed for monopole transitions, due to the difficulty of treating the two-center continuum states [13, 14].

When the collision velocity v is much less than the electron orbiting velocity in its initial state, united-atom perturbation theory will be applicable [15]. Thereby, the two-center energies and wavefunctions

are replaced by time-independent functions at the united atom [16] or rather at the distance of closest approach [17]. Within this prescription, it is easy to include transitions of higher multipolarity in order to get a correct description of the electronic angular distribution. In the following section we apply the Briggs model to calculate the electron emission from the K and L shell of relativistic atoms, including multipole transitions up to $l=2$. In Sect. 3 the properties of the angular distribution are discussed and a comparison with experiment is given for the collision of S with Pb.

2. Theory

The formalism developed for the atomic perturbation theory [11] is readily applied to the case of united-atom perturbation theory. As a detailed description is given in [17], we confine ourselves to a short outline of the theory. In first-order perturbation theory, the transition amplitude for exciting an electron from the initial state ψ_i with energy E_i to a final continuum state ψ_f with energy E_f is given by [15]

$$a_{fi} = \frac{1}{i\hbar} \int_{-\infty}^{\infty} dt \langle \psi_f | \left(-\frac{Z_1 e^2}{|\mathbf{r} - \alpha \mathbf{R}|} - \frac{Z_2 e^2}{|\mathbf{r} + \beta \mathbf{R}|} \right) |\psi_i\rangle$$
$$\cdot e^{i(E_f - E_i)t/\hbar} \tag{2.1}$$

where the center of charge frame is chosen as reference system for the electron, such that $\alpha = Z_2/(Z_1 + Z_2)$ and $\beta = 1 - \alpha$ where Z_1 and Z_2 are the charges of the projectile and target nucleus, respectively. The internuclear motion $\mathbf{R}(t)$ is described by the classical Rutherford trajectory. The evaluation of (2.1) proceeds with the help of a Fourier transformation of the interaction field $V(t)$ and a partial wave decomposition of both $V(t)$ and the final state ψ_f. One thereby achieves a separation of coordinate and time integrals in momentum space. While the coordinate integral, yielding the form factors, can be done analytically for (relativistic) hydrogenic wavefunctions, the path factors from the time integral

$$B_{lm}(q) = \int_{-\infty}^{\infty} dt \, e^{i(E_f - E_i)t/\hbar} j_l(qR) Y_{lm}^*(\hat{\mathbf{R}}) \tag{2.2}$$

where j_l is a Bessel function, can only be evaluated analytically for angular momenta $l \leq 1$ in case of a hyperbolic trajectory [11]. It has been shown, however, that for large scattering angles the hyperbolic path can be approximated by a zero-impact parameter broken-line path [10, 18], leading to simple formulas for B_{lm} [18, 11]. If, instead, the hyperbola is replaced by its asymptotes (i.e. keeping the dis-

tance of closest approach finite), the range of validity is extended to small scattering angles and thus to the calculation of total cross sections. In addition, the velocity may be modified in order to account for retardation [19]. We have applied this prescription for the evaluation of the B_{2m} only (see Appendix).

With an analytic approximation of $B_{lm}(q)$, only the integral over the momentum transfer q has to be done numerically. The transition probability for ejecting an electron with energy E_f into the solid angle $d\Omega_f$ can then be written in terms of a multipole expansion [17]

$$\frac{d^2 P(b)}{dE_f d\Omega_f} = \sum_{\lambda\mu} p_{\lambda\mu}(b, E_f) Y_{\lambda\mu}(\Omega_f). \tag{2.3}$$

Retaining multipoles up to $\lambda = 2$, (2.3) may be written in the form

$$\frac{d^2 P(b)}{dE_f d\Omega_f} = M_0(b) + D_0(b) \cos\vartheta_f + D_1(b) \sin\vartheta_f \cos\varphi_f$$
$$+ Q_0(b)(3\cos^2\vartheta_f - 1)$$
$$+ Q_1(b) \cos\vartheta_f \sin\vartheta_f \cos\Omega_f.$$
$$+ Q_2(b) \sin^2\vartheta_f \cos 2\varphi_f. \tag{2.4}$$

The impact parameter $\mathbf{b}$, which enters into the path $\mathbf{R}(\mathbf{b}, t)$ and thus into B_{lm}, defines the x-axis (being perpendicular to $\mathbf{v}$ which is chosen as z-axis). As the transition probability is a scalar, the azimuthal angle φ_f is just the angle between $\mathbf{b}$ and $\mathbf{k}_{f\perp}$ where $\mathbf{k}_{f\perp}$ is the projection of the electron momentum $\mathbf{k}_f$ into the (x, y) plane. Thus, for studying the dependence of the intensity of the emitted electrons on φ_f, it is necessary to specify the scattering plane, i.e. observe the direction of the scattered projectile.

In order to obtain the cross section, one has to integrate over $\mathbf{b}$. Then the terms with $\mu \neq 0$ vanish such that

$$\frac{d^2\sigma}{dE_f d\Omega_f} = \int_0^\infty b \, db \int_0^{2\pi} d\varphi_f \frac{d^2 P(b)}{dE_f d\Omega_f}$$
$$= M_0 + D_0 \cos\vartheta_f + Q_0(3\cos^2\vartheta_f - 1). \tag{2.5}$$

In the following section we demonstrate that it is sufficient to retain only terms with $\lambda \leq 1$ as long as E_f is much larger than the binding energy of the initial state, due to the great momentum transfer required for the ejection of these electrons. However, even for slow collisions, quadrupole transitions modify the angular distribution considerably when E_f is small.

3. Numerical Results

We have calculated the angular dependence of the δ-electrons ejected from the K and L shell in the collisions of S and Ni with Pb, at a projectile energy

of 150 MeV and 343 MeV, respectively, corresponding to a ratio of $\hbar v/(Z_1+Z_2)e^2=0.14$. We have used hydrogenlike wavefunctions with an impact-parameter dependent effective charge and b-dependent binding energies to approximate the molecular wavefunctions and energies at the distance of closest approach, $R_0(b)$, following the prescription given in [17]. For reasons of consistency, we have restricted the multipole terms from the partial wave expansion of the interaction field to $l\leq2$, when calculating the angular distribution including $\lambda\leq2$. The accuracy of the calculations is about 5 %.

It has been shown in [17] that ionisation of the $2s_{1/2}$ state gives the dominant contribution to the δ-electrons for the presently investigated collision systems, as long as the electron energy E_f is not much lower than the L-shell binding energy. Therefore, we restrict the discussion mainly to this state.

Figure 1 displays the influence of quadrupole transitions on the differential cross section as a function of the energy E_f of the emitted electrons. While the inclusion of $l=2$ yields a contribution of only 10 % for the *angular integrated* cross section, i.e. the term M_0 in (2.5), at the lowest energies, it is of considerable importance for the angular distribution at small E_f. Even the dipole term D_0 which determines the forward-backward asymmetry of the ejected electrons, is largely modified at the lower E_f when quadrupole transitions are included. However, when E_f approaches the (united-atom) binding energy, the ratio Q_0/M_0 drops rapidly, and the changes of D_0 become smaller.

It is further seen from Fig. 1 that there is a minimum of D_0 around $E_f\approx10-20$ keV, which means that the ejection of electrons into the forward direc-

tion is strongly suppressed, and may even be smaller than in the backward direction. This feature is the more pronounced, the higher the combined charge of the system, and origins both from the behaviour of the path factor B_{10} and from the phase shifts entering into the terms $P_{\lambda\mu}$ $(\lambda\neq0)$ in (2.3) which at this energy add in such a way that the dipole term changes sign. On the other hand, D_0 decreases when Z_1/Z_2 becomes larger [17], as the contributions from the projectile and target field tend to cancel each other, such that for the visibility of this effect in experiments both Z_2/Z_1 and Z_1+Z_2 have to be large.

In order to estimate the reliability of the broken-line approximation we have used (A.7) also for the calculation of the monopole and dipole path factors. We found that (A.7) is a good approximation to the exact B_{00} and B_{10}, especially at large impact parameters (the change in the differential cross section lies in the percent region), however, the broken-line formula is not so safe for B_{11}, leading to an increase of Q_0/M_0 by about 10 % for small E_f. Nevertheless, with (A.7) the shape of Q_0/M_0 and D_0/M_0 is very close to the one shown in Fig. 1. Therefore we do not expect a qualitative different behaviour if B_{2m} is replaced by the Rutherford formula, except that the quadrupole contribution may be somewhat lower at small E_f.

Figure 2 shows the coefficients $M_0(b)$ and $D_\mu(b)$ at

Fig. 1. Multipole contributions M_0, D_0 and Q_0 to the electron emission cross section from the $2s_{1/2}$ state as a function of electron energy E_f. The full curves correspond to a 150 MeV (S, Pb) collision and the dash-dotted curves are for a 343 MeV (Ni, Pb) collision (quadrupole $l=2$ included). The dashed curve is the $l\leq1$ contribution only for (S, Pb)
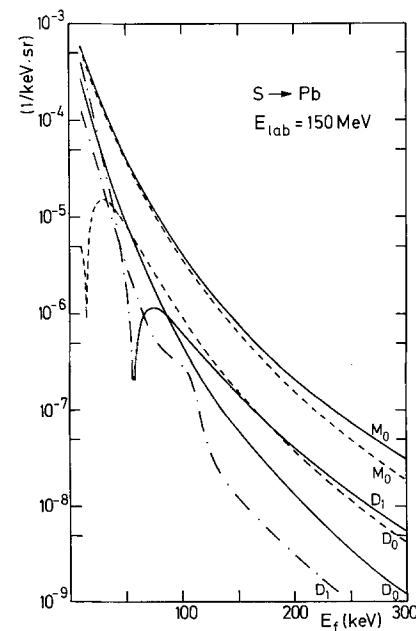

Fig. 2. Coefficients M_0, D_0 and D_1 for the transition probability of $2s_{1/2}$ electrons as a function of the energy E_f. The full curves belong to an impact parameter $b=9.5$ fm $(\vartheta=75.3°)$, the dashed curves are for $b=56$ fm $(\vartheta=14.7°)$. Dash-dotted curves denote a negative sign

fixed impact parameter as a function of the electron energy. While the monopole term decreases smoothly with E_f for any b, the dipole terms change sign. The cause for D_1 being negative at large b and positive at small b (for large E_f where the phase shifts depend weakly on E_f) lies in the path factor B_{11} and thus only in the collision dynamics. A positive coefficient of $\cos\varphi_f$ indicates that more electrons are ejected into the half-space where the path of the scattered projectile is lying (extending from $\varphi = -\pi/2$ to $+\pi/2$ in Fig. 3). Thus at large ϑ the electrons are preferrably ejected into the neighbourhood of the projectile because of the strong attraction in close collisions, while for small scattering angles the electrons rather follow the target
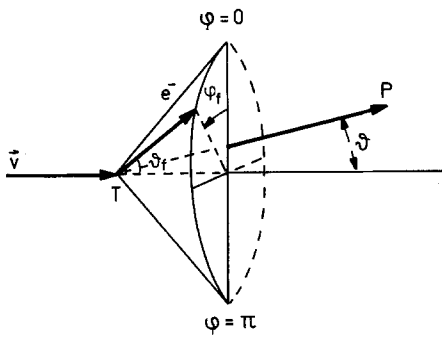
Fig. 3. Coordinate system showing the direction of the incoming and scattered projectile (P) as well as the angles of the emitted electron (e^-)
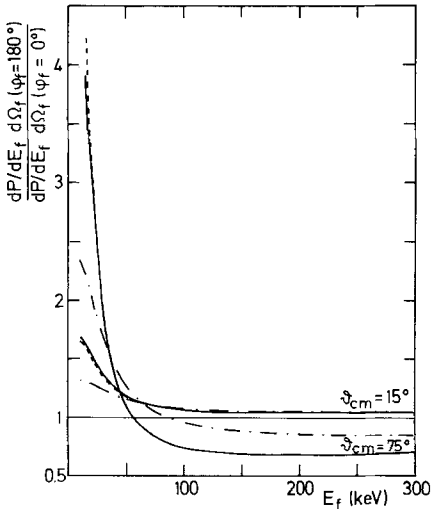
Fig. 4. Ratio of transition probabilities for the $2s_{1/2}$ electrons emitted at $\vartheta_f = 90°$ and $\varphi_f = 180°$ and $0°$ as a function of energy E_f. Shown are the ratios at two different impact parameters $b \approx 55$ fm ($\vartheta \approx 15°$) and $b \approx 9$ fm ($\vartheta \approx 75°$). Full curves are for 150 MeV (S, Pb) collisions and dash-dotted curves are for 343 MeV (Ni, Pb) collisions. The dashed curves are calculated for a S projectile without $l = 2$ transitions

(which moves in the opposite half-space in the center of mass frame), and do not change much their initial direction.

This dependence on φ_f is more clearly displayed in Fig. 4, where the ratio $R = d^2 P(\varphi_f = 180°)/d^2 P(\varphi_f = 0°)$ determining the anisotropy of the electrons at a fixed emission angle ($\vartheta_f = 90°$, where the effect is largest) is shown. Although the sign of $R - 1$ is mainly determined by D_1, its magnitude is approximately given by the ratio of D_1/M_0 which is mostly smaller for the less asymmetric collision system (Ni, Pb) than for (S, Pb). For scattering angles $\vartheta \lesssim 20°$, the anisotropy is much smaller than at larger ϑ. Below the energy region around 50 keV, there is a steep rise of the anisotropy, simply reflecting the fact that a great deal of the slow electrons keep close to the target atom.

Recently, pioneer experiments with 147 MeV S colliding with Pb have been performed by Koenig and coworkers [4] which allow for a determination of all four quantities b, E_f, ϑ_f and φ_f. In Fig. 5 the transition probability $d^2 P/dE_f d\Omega_f$ at $\vartheta_f = 100°$ is shown when integrated over φ_f from $\pi/2$ to $3\pi/2$ on one hand and from $-\pi/2$ to $\pi/2$ on the other hand. As the experimental data do not specify the initial state we have summed the contributions from the K and L shells. For $E_f = 200$ keV, the K-shell probability
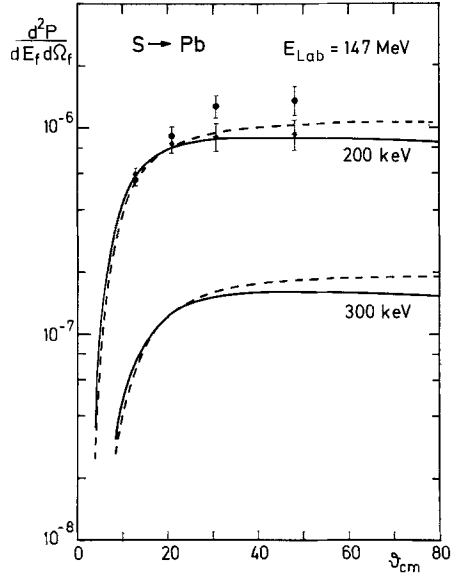
Fig. 5. Scattering angle dependence of the electron emission probability in 147 MeV (S, Pb) collisions at the emission angle $\vartheta_f = 100°$. The calculation is a sum over K and L shell contributions, and $l = 2$ is included for the $2s_{1/2}$ state. The full curves and ♦ denote the φ_f integration regime from $\pi/2$ to $3\pi/2$, the broken curves and ♠ are for φ_f between $-\pi/2$ and $\pi/2$. The data are from Koenig and coworkers [4] and include electron energies in the region 200–330 keV.

amounts already to about 1/3 of the total probability, except at very small scattering angles (<10°). The crossing of the curves through the data points for the two φ_f regions, i.e. the change of sign in the anisotropy, lies slightly below $\vartheta = 20°$ and is in agreement with the theoretical predictions. Also the magnitude of the anisotropy as a function of scattering angle is very similar in theory and experiment, and depends only weakly on E_f in this high-energy region.

The deviation of the angular distribution from an isotropic one for the $2s_{1/2}$ initial state (or the $1s_{1/2}$ state which behaves similarly) is mainly due to the collision dynamics, as the velocity $\mathbf{v}$ specifies a certain direction. On the other hand, anisotropies of a different kind are expected for the $2p$ states. It follows from momentum conservation that electrons which are emitted into the direction $\hat{\mathbf{k}}_f$ had initially a momentum $\mathbf{p}$ which is the closer to $\mathbf{k}_f$, the larger E_f and the smaller v. For the $2p$ states, the asym-

metry of the $\mathbf{p}$ distribution (given by the wavefunction) is thus visible in the angular distribution of the emitted electrons. In Fig. 6 the probability $d^2P/dE_f d\Omega_f$ for electron emission from the L subshells is plotted as a function of φ_f and ϑ_f, respectively. Both E_f (200 keV) and b ($\vartheta = 15°$) were chosen to be large in order to reduce the anisotropies arising from the collision dynamics. In contrast to the periodicity π of the angular distribution of Auger electrons or x-rays which results from the production via a two-step process [7], and which allows for a direct image of the density distribution in the initial state, the δ-electrons have only the periodicity 2π. This reflects the close coupling between structural and dynamical effects. In the plane $\varphi_f = 0$ (i.e. the scattering plane, cf. Fig. 3) the direction of maximal intensity does not coincide with the direction of $\mathbf{v}$, but is dependent on impact parameter (the symmetry axis is denoted by a dashed line). While, as discussed previously, this direction changes by more than 200° for the $2s_{1/2}$ state when b varies from 0 to ∞, it is rather stable (changes less than 50°) for the $2p_{1/2}$ and $2p_{3/2}$ states. Furthermore, the difference in the direction of maximal intensity between the $2p_{1/2}$ and $2p_{3/2}$ states is always near 180°. This is a clear indication for the influence of the electronic wavefunctions on the angular distribution.

In conclusion, by means of a calculation based on the semiclassical description and first-order united-atom perturbation theory, we have demonstrated that the δ-electrons emitted from the inner shells of relativistic atoms show a pronounced angular dependence even for collision velocities which are much lower than the electron velocity in the initial shell, provided the asymmetry Z_2/Z_1 of the collision system is large. If in addition to the polar angle ϑ_f of the electrons, the azimuthal angle φ_f is observed (at fixed impact parameter), a distinct anisotropy with respect to the emission at $\varphi_f = 0°$ and $\varphi_f = 180°$ is found. For 150 MeV (S, Pb) collisions, it amounts up to some 10 %, being somewhat lower for the (Ni, Pb) system at the scaled velocity. It has been shown that the ϑ_f, φ_f distribution is closely related to both the structure of the initial state as well as to the collision dynamics. In particular, for electron energies near the initial binding energy, the angular distribution is strongly influenced by the relative phases of the partial wave terms in the transition amplitude, which thus are accessible to experimental investigation.
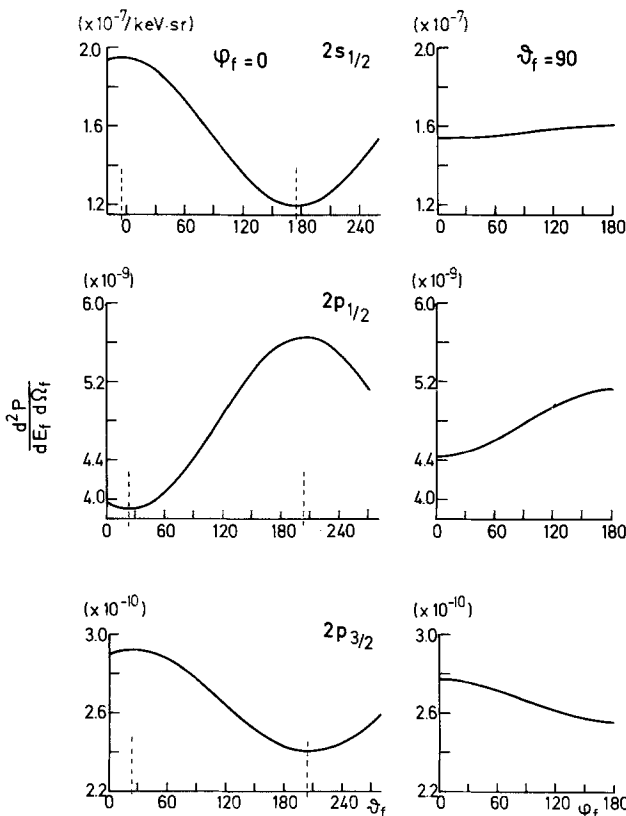
Fig. 6. Probability $d^2P/dE_f d\Omega_f$ for emission of 200 keV electrons in 150 MeV (S, Pb) collisions at an impact parameter $b = 56$ fm ($\vartheta = 14.7°$) from the $2s_{1/2}$, $2p_{1/2}$ and $2p_{3/2}$ state. Only dipole transitions ($l \leq 1$) are included. The probability is shown at $\varphi_f = 0$ as a function of ϑ_f (left) and at $\vartheta_f = 90°$ as a function of φ_f (right)

Appendix

We evaluate the path factors B'_{lm} in a coordinate system (denoted by a prime) where the x-axis is chosen as symmetry axis of the internuclear path, i.e. pointing along $\mathbf{R}(t)$ at $t=0$, while the z-axis is perpendicular to it, forming the angle $\vartheta/2$ with the velocity $\mathbf{v}$ (ϑ is the scattering angle). We approximate the Rutherford hyperbola by its asymptotes

$$\mathbf{R} = b_0\, \mathbf{e}_x + (\mp \sin\vartheta/2\, \mathbf{e}_x + \cos\vartheta/2\, \mathbf{e}_z)vt, \quad t \lessgtr 0$$

$$b_0 = \frac{b}{\cos\vartheta/2} \tag{A.1}$$

where the smallest distance from the z-axis, b_0, is kept finite. For $b_0 = 0$, this is the broken-line path from [18]. For large impact parameters b, i.e. $\vartheta \to 0$, (A.1) becomes the straight-line path for the correct impact parameter, which is not the case if $b_0 = 0$. Thus, (A.1) is also a reasonable approximation for small scattering angles, and can be used for the calculation of total cross sections.

For the evaluation of B_{lm} defined in (2.2) it is convenient to write the $\mathbf{R}$ dependence in an exponential form by means of the relation

$$j_l(qR)\, Y_{lm}(\hat{\mathbf{R}}) = \frac{1}{4\pi} i^{-l} \int d\Omega_q\, e^{i\mathbf{q}\mathbf{R}}\, Y_{lm}(\hat{\mathbf{q}}) \tag{A.2}$$

which can be obtained from a partial wave expansion of $\exp(i\mathbf{q}\mathbf{R})$ and implies the same quantisation axis for $\hat{\mathbf{q}}$ and $\hat{\mathbf{R}}$. In order to cast the dependence on ϑ into a simple form we rotate $\mathbf{q}$ through an angle $\vartheta/2$ which corresponds to choosing a new z-axis along $\mathbf{v}$

$$q'_z = \mp \sin\vartheta/2\, q_x + \cos\vartheta/2\, q_z$$
$$q'_x = \cos\vartheta/2\, q_x \pm \sin\vartheta/2\, q_z \qquad t \lessgtr 0 \tag{A.3}$$

Under this rotation, the spherical harmonics are transformed by means of the rotation matrix $d^l_{m'm}(\pm\vartheta/2)$ [20] such that B'_{lm} is found from

$$B'_{lm}(q) = \frac{1}{4\pi} i^{-l} \int d\Omega_{q'} \sum_{m'} Y_{lm'}(\hat{\mathbf{q}}')$$

$$\left[d^l_{m'm}(-\vartheta/2) e^{ib_0(\cos\vartheta/2\, q'_x - \sin\vartheta/2\, q'_z)} \int_{-\infty}^{0} dt\, e^{i\Delta Et}\, e^{iq'_z vt} \right.$$

$$\left. + d^l_{m'm}(\vartheta/2) e^{ib_0(\cos\vartheta/2\, q'_x + \sin\vartheta/2\, q'_z)} \int_{0}^{\infty} dt\, e^{i\Delta Et}\, e^{iq'_z vt} \right] \tag{A.4}$$

with $\Delta E = (E_f - E_i)/\hbar$. The time integral is straightforward, and when spherical coordinates are used, also the integral over $\varphi_{q'}$ is easily carried out:

$$\int_{0}^{\infty} dt\, e^{\pm i(\Delta E + q'_z v)t} = \pi\, \delta(\Delta E + q'_z v) \pm \frac{i}{\Delta E + q'_z v}$$

$$\int_{0}^{2\pi} d\varphi_{q'}\, e^{ib_0 \cos\vartheta/2\, q \sin\vartheta_{q'} \cos\varphi_{q'} + im'\varphi_{q'}} \tag{A.5}$$

$$= 2\pi\, i^{|m'|}\, J_{|m'|}(b_0 \cos\vartheta/2\, q \sin\vartheta_{q'})$$

where J_m is a Bessel function. Using further the symmetry properties of the rotation matrices, B'_{lm} can be written as a sum of two terms, the first of which is proportional to the δ-function in (A.5) which makes the integration over $x = \cos\vartheta_{q'}$ trivial

$$B'_{lm} = B'^{(1)}_{lm} + B'^{(2)}_{lm}$$

$$B'^{(1)}_{lm} = \frac{\pi}{2qv} i^{-l} \sum_{m'=-l}^{l} i^{|m'|}\, Y_{lm'}\left(\arccos\frac{\Delta E}{qv}, 0\right)$$

$$\cdot (-1)^{l+m'} J_{|m'|}(b\sqrt{q^2 - (\Delta E/v)^2})\, d^l_{m'm}(\vartheta/2)$$

$$\cdot \left[(-1)^{m-m'} e^{i\frac{\Delta E}{v}b\tan\vartheta/2} + e^{-i\frac{\Delta E}{v}b\tan\vartheta/2} \right]$$

$$\cdot \theta(q - \Delta E/v)$$

$$B'^{(2)}_{lm} = \tfrac{1}{2} i^{-l+1} \sum_{m'=-l}^{l} i^{|m'|} \sqrt{\frac{(2l+1)(l-m')!}{4\pi(l+m')!}}$$

$$\cdot d^l_{m'm}(\vartheta/2) \int_{-1}^{1} dx\, P_l^{m'}(x) \frac{1}{\Delta E + qvx}$$

$$\cdot J_{|m'|}(bq\sqrt{1-x^2})[-(-1)^{m-m'} e^{-iqbx\tan\vartheta/2}$$

$$+ e^{iqbx\tan\vartheta/2}] \tag{A.6}$$

where θ is the unit step function. In the limiting case of a straight line ($\vartheta = 0$) with impact parameter b, $d^l_{m'm} = \delta_{m'm}$ such that $B'^{(2)}_{lm}$ vanishes and the straight-line path factors [11] are recovered. On the other hand, when b is set equal to zero (but ϑ is kept finite), the only contribution comes from $m' = 0$ where $d^l_{m'm}$ becomes proportional to $Y_{lm}(\vartheta/2, 0)$, and the broken-line result from [18] is obtained. However, if the relation $b = d\cot\vartheta/2$ for a hyperbolic path is inserted ($d = Z_1 Z_2 e^2/(\mu v^2)$, μ being the reduced mass), the phases $\sim b\tan\vartheta/2$ become independent of ϑ and (A.6) differs from the straight-line and broken-line result for $\vartheta \to 0$ ($b \to \infty$) and $\vartheta \to \pi$ ($b \to 0$), respectively, by a factor $\cos\alpha_0$ with $\alpha_0 \sim d\Delta E/v$, including terms $\sim \sin\alpha_0$ which are not present in the two asymptotic theories. Note that terms involving α_0 do also appear in the Coulomb deflection factor [8, 19]. For our cases of interest, α_0 will mostly be small. We have found that for high electron energies, the broken-line formula from [18] describes the impact-parameter distribution well for all b except for very large ones where $d^2 P(b)/dE_f d\Omega_f$ has already decreased to a small value. Thus we use a simple analytic modification of

the broken-line formula implied by the structure of (A.6):

$$B'_{lm}(q) = \frac{\pi i^l}{qv} Y_{lm}(\vartheta/2, 0) P_l(\Delta E/qv)$$

$$\cdot J_0(b\sqrt{q^2 - (\Delta E/v)^2})\,\theta(q - \Delta E/v), \quad m \text{ even}$$

$$B'_{lm}(q) = \frac{2 i^{l+1}}{qv} Y_{lm}(\vartheta/2, 0) Q_l(\Delta E/qv)$$

$$\cdot \begin{cases} J_0(b\sqrt{q^2 - (\Delta E/v)^2}), & q \geq \Delta E/v \\ J_0(bq\sqrt{1 - (qv/\Delta E)^2}), & q < \Delta E/v \end{cases}, \quad m \text{ odd}$$

$$(A.7)$$

where Q_l is a Legendre function of the second kind. (A.7) differs from the zero-impact parameter broken-line result only through the Bessel function J_0 which ensures that B'_{lm} and thus the transition probability vanishes in the limit $b \to \infty$. For $l = 0$, (A.7) reduces to the straight-line result.

Besides the Coulomb deflection, the retardation can be easily incorporated into (A.7) by choosing an impact-parameter dependent velocity [19]

$$v \to v' = \frac{v}{2}\left(1 + \frac{b}{d + \sqrt{b^2 + d^2}}\right). \quad (A.8)$$

In our calculation, (A.7) with (A.8) is used only for $l = 2$, while for $l \leq 1$, B'_{lm} is taken from [11, 17]. In order to obtain the path factors in a coordinate frame with the (initial) projectile velocity **v** as quantisation axis, which is the natural one for comparison with experiments, all B'_{lm} have to be rotated by means of

$$B_{lm}(q) = \sum_{m'} d^l_{m'm}(\vartheta/2) B'_{lm'}(q). \quad (A.9)$$

References

1. Kozhuharov, C., Kienle, P., Jakubaßa, D.H., Kleber, M.: Phys. Rev. Lett. **39**, 540 (1977)
2. Bosch, F., Krimm, H., Martin, B., Povh, B., Walcher, Th., Traxel, K.: Phys. Lett. **78**B, 568 (1978)
3. Güttner, F., Koenig, W., Martin, B., Povh, B., Skapa, H., Soltani, J., Walcher, Th., Bosch, F., Kozhuharov, C.: Z. Phys. A - Atoms and Nuclei **304**, 207 (1982)
4. Koenig, W.: Private communication (1983)
5. Jitschin, W., Kleinpoppen, H., Hippler, R., Lutz, H.O.: J. Phys. B**12**, 4077 (1979)
6. Kessel, Q.C., Morgenstern, R., Müller, B., Niehaus, A.: Phys. Rev. A**20**, 804 (1979)
7. Eichler, J., Fritsch, W.: J. Phys. B**9**, 1477 (1976)
8. Bang, J., Hansteen, J.M.: Dan. Vidensk. Selsk. Mat.-Fys. Medd. **31** (No 13) (1959)
9. Choi, B.H., Merzbacher, E.: Phys. Rev. **177**, 233 (1969)
10. Aashamar, O., Kocbach, L.: Z. Phys. A - Atoms and Nuclei **279**, 237 (1976)
11. Amundsen, P.A.: J. Phys. B**11**, 3197 (1978)
12. Pauli, M., Rösel, F., Trautmann, D.: J. Phys. B**11**, 2511 (1978)
13. Soff, G., Greiner, W., Betz, W., Müller, B.: Phys. Rev. A**20**, 169 (1979)
14. Soff, G., Reinhardt, J., Müller, B., Greiner, W.: Z. Phys. A - Atoms and Nuclei **294**, 137 (1980)
15. Briggs, J.S.: J. Phys. B**8**, L485 (1975)
16. Amundsen, P.A.: J. Phys. B**11**, L737 (1978)
17. Jakubaßa-Amundsen, D.H.: Phys. Scr. **26**, 319 (1982)
18. Andersen, J.U., Kocbach, L., Laegsgaard, E., Lund, M., Moak, C.D.: J. Phys. B**9**, 3247 (1976)
19. Kocbach, L.: Phys. Norv. **8**, 187 (1976)
20. Edmonds, A.R.: Drehimpulse in der Quantenmechanik. p. 75. Mannheim: BI 1964

D.H. Jakubaßa-Amundsen
Physik-Department
Technische Universität München
James-Franck-Strasse
D-8046 Garching bei München
Federal Republic of Germany